Supplementary Material

Cytosolic pH is a second messenger for glucose and regulates the PKA pathway via V-ATPase

Reinhard Dechant, Matteo Binda, Sung Sik Lee, Serge Pelet, Joris Winderickx and Matthias Peter

Table S1: Yeast strains used in this study.

Strain No	Relevant genotype	Source
BY4741 (wild-type)	MATa *ura3Δ0; leu2Δ0; his3Δ1; met15Δ0*	Openbiosystems
RD66	*VMA5-GFP::HIS3*	Openbiosystems
RD68	*VPH1-GFP::HIS3*	Openbiosystems
RD146	*VMA5-RFP::KAN^R*	This study
RD157	*VMA5-RFP::KAN^R; VPH1-GFP::HIS3*	This study
RD67	*VMA2-GFP::HIS3*	Openbiosystems
RD148	*VMA5-RFP::KAN^R*	This study
RD151	*VMA5-RFP::KAN^R pHluorin::URA3*	This study
RD57	*vma5Δ::KAN^R*	Openbiosystems
RD152	*vma5Δ::KAN^R; pHluorin::URA3*	Openbiosystems
RD155	*VPH1-WT::URA3; VMA5-RFP::KAN^R*	This study
RD156	*VPH1-D329N::URA3; VMA5-RFP::KAN^R*	This study
RD105	*cdc19-1ts::KAN^R*	C. Boone
RD78	*pgm2Δ::KAN^R*	Openbiosystems
RD58	*ppa1Δ::KAN^R*	Openbiosystems
RD59	*vma2Δ::KAN^R*	Openbiosystems
RD98	*gpa2Δ::NAT^R*	This study
RD159	*vma5Δ::KAN^R; gpa2Δ::NAT^R*	Openbiosystems
RD116	*pHSP12-qV-LEU2::HSP12*	This study
RD118	*pHSP12-qV-LEU2::HSP12; vma5Δ::KAN^R*	This study
RD120	*pHSP12-qV-LEU2::HSP12; vma2Δ::KAN^R*	This study
RD121	*pHSP12-qV-LEU2::HSP12; gpa2Δ::NAT^R*	This study
RD122	*pHSP12-qV-LEU2::HSP12; vma2Δ::KAN^R; gpa2Δ::NAT^R*	This study
RD142	*W303 pHSP12-qV::LEU2*	This study
RD144	*W303 pHSP12-qV::LEU2; msn2Δ::NAT^R; msn4Δ::NAT^R*	This study
RD74	*VMA5-GFP::HIS3; ira2Δ::KAN^R*	This study

Table S2: Plasmids used in this study.

Plasmid No	Genotype	Source
pCB901YpHc	YCPlac111-pHSP-pHluorin	R. Rao
pRD21	pRS316-pGPD-pHluorin	This study
pRD22	pRS306-pGPD-pHluorin	This study
pRD25	Msn2p-NLS-GFP (pPKI-NES-Msn2p(567-704)-GFP) *LEU2*	Gorner et al., 2002
pRD14	pRS306-*VPH1*	This study
pRD15	pRS306-*VPH1-D329N*	This study
pSP29	pRS305 pHSP12-qV (4x YFP/Venus)	S. Pelet
pSP83	Msn2p-GFP *LEU2*	Gorner et al., 2002
pGEX2T-RBD	GST-Raf-1 (1-149)	Colombo et al, 2004

Table S3: V-ATPase reassembly can be triggered by addition of various hexoses, but not glycerol or pyruvate to starved cells.

	Pre-grown prior to starvation in	
C-source added	Glucose	Galactose
Glucose	+++	+++
Fructose	+++	+++
Galactose	-	+++
Glycerol	-	-
Pyruvate	-	-
Fucose	n.d.	-
2-deoxy-glucose	-	n.d.

Table S4: Hydrolysis of ATP and reduction of NAD+ produces H^+.

Reaction	inferred pH change
$ATP \rightarrow ADP + P_i + H^+$	decrease
$NAD^+ \rightarrow NADH + H^+$	decrease

Supplementary Table legends:

Table S3: V-ATPase reassembly can be triggered by addition of various hexoses, but not glycerol or pyruvate to starved cells.

Summary of time-lapse analysis of V-ATPase reassembly in starved cells after addition of different carbon sources. Cells were pre-grown in synthetic complete medium containing glucose or galactose as indicated. Reassembly was scored 4 min after addition of carbon source. Note that cells grown in glucose do not express transporters and enzymes required for the utilization of galactose and thus do not respond to galactose stimulation within the analyzed time frame.

Table S4: Hydrolysis of ATP and reduction of NAD+ produces H^+.

Chemical reactions for hydrolysis of ATP and reduction of NAD^+. Both reactions generate protons. Thus, shifting the balance towards more ATP hydrolysis and/or NAD^+ reduction should contribute to a decrease of cytosolic pH, yet the absolute contribution to the changes in pH remains to be determined.

Supplementary Figure legends:

Supplementary Figure S1: Regulation of V-ATPase and cytosolic pH by glucose.

(A) Schematic representation of the microfluidic chips used in the study. Cells are trapped in a cell chamber (Y2, Cellasics Corp.) connected with two inlets for growth medium to allow fast switch between two different media (e.g. with glucose, or C-starvation). Flow of media is controlled by application of air pressure using an automated pressure controller (ONIX, Cellascic Corp.). Exchange of medium is followed by addition of a fluorescent dye to the growth media. Cells are loaded by

increasing flow rate leading to dilation of the cell chamber and allowing the cells to enter the cell chamber. Upon reduction of flow, cells are mechanically fixed in position throughout the experiment. (B) Quantification of V-ATPase assembly using automated image analysis. See Methods for details. (C) Validation of automated quantification of V-ATPase assembly. Time-lapse analysis of V-ATPase assembly in cells expressing Vma5p-RFP and Vph1p-GFP. V-ATPase assembly is quantified as in Figure 1C and plotted as the mean +/- SEM as a function of time. Strong disassembly is observed for Vma5p-RFP, while localization of Vph1p remains unaffected upon starvation, leading to little change in the relative CV of the Vph1p-GFP signal. (D) Regulation of V-ATPase by glucose in cells expressing Vma2p-GFP. Cells were grown in SD and starved for glucose for 15 min in a microfluidic chamber. Representative images and automated quantification of V-ATPase assembly are shown. (E) Cytosolic pH is regulated by glucose, but independent of V-ATPase activity. Cells were grown in YPD, starved and processed for SNARF-4 staining. Cells were resuspended in SC and pH was measured by ratio imaging under the fluorescence microscope 10 min after addition of glucose. Data are represented as average +/- σ of at least three independent experiments. Asterisks indicate P values obtained from a *t*-test of $P < 0.02$ (*) and $P < 0.001$ (**) relative to the starved cells of the same condition/genotype. In each individual experiment, more than 40 cells were scored per condition.

Supplementary Figure S2: V-ATPase activity is unaffected in cells expressing *vph1-D329N*

(A) Quinacrine staining of wild-type and *vph1-D329N* cells. (B) Serial dilutions of cells spotted on yeast media as indicated are shown. Cells deleted for *VPH1* and *VMA5* are included for control.

Supplementary Figure S3: Localization of Msn2p-NLS-GFP is regulated by glucose, but independent of TORC1 activity.

(A) Schematic representation of functional domains of the Msn2p and Msn2p-NLS constructs used in this study (adapted from Gorner et al, 2002). NLS: Nuclear localization signal, NES: Nuclear export signal, ZnF: Zinc-finger. Serines (S) that are phosphorylated by PKA in the NLS are indicated. S582 used in Figure 4 is highlighted in red. (B) Cells expressing Msn2p-NLS-GFP were grown in SD medium, starved for 10 min or treated with Rapamycin (200ng/l) for 15 min. Representative images of cells are shown.

Supplementary Figure S4: Expression of *HSP12* is dependent on Msn2p and Msn4p and regulated by V-ATPase.

(A and B) Wild-type (grey) and *msn2*Δ*;msn4*Δ (red) cells harboring the *pHSP12-qV* reporter were grown to early log phase (A) or until the entry of the diauxic shift (when PKA activity is reduced) (B). Expression of the fluorescent reporter was scored by FACS and representative histograms are shown. (C and D) *HSP12* expression is derepressed in *vma5*Δ cells. Cells of the indicated genotype expressing the p*HSP12-qV* reporter were grown in SD media +/- 20mM cAMP and 25000 cells were scored as in (A). (C) Representative histograms and (D) quantification of 5 independent experiments, represented as the mean +/- σ relative to wild-type, are shown. (E) Cells of the indicated genotype harboring the *HSP12*-YFP reporter were grown SD media and scored in triplicates as in (A). A representative result of three independent experiments is shown as mean +/- σ relative to wild-type.

Supplementary Figure S5: V-ATPase and Gpa2p cooperatively regulate cell growth.

(A) Representative tetrads from dissections of diploid cells with heterozygous deletions of V-ATPase components (yellow) and *GPA2* (red). (B) Summary of the genetic interactions described in this study. Dashed line: synthetic sickness; solid line: synthetic lethality. (C) Meta analysis of published literature data on genetic interactions of genes involved in the Ras/PKA and V-ATPase assembly and function. Data were retrieved form the DRYGIN database and displayed as a heatmap (generated by Treeview (Page, 1996); red positive genetic interaction, green negative genetic interaction) and as a genetic network (generated by Cytoscape (Shannon et al, 2003)); red: interactions between components of V-ATPase, blue: interactions between components of the Ras/PKA pathway and green interactions between components of V-ATPase and the Ras/PKA pathway.

Supplementary Figure S6: V-ATPase disassembly upon starvation is not affected by deletion of the Ras-GAP *IRA2.*

(A and B) Cells of the indicated genotypes expressing Vma5p-GFP were grown and starved for glucose. (A) Representative images and (B) automated quantification of V-ATPase assembly of cells before or 15 min after glucose starvation are shown. Data are mean +/- SEM.

Supplementary Figure S7: Hypothetical model for pH regulation by glucose metabolism.

Model depicting the potential contributions of metabolism and the P-ATPase in the regulation of cytosolic pH and V-ATPase regulation and convergence of different activators on adenylate cyclase activity. Possible interactions of V-ATPase

with the Ras/PKA pathway explaining the observed phenotypes are indicated with blue dashed arrows. Proposed positive feed-back loop from PKA to V-ATPase assembly, possibly explaining published data on defects in V-ATPase disassembly in cells deleted for *IRA2*, is indicated with a red dashed arrow. See discussion for details. glc: glucose.

Supplementary references:

Gorner W, Durchschlag E, Wolf J, Brown EL, Ammerer G, Ruis H, Schuller C (2002) Acute glucose starvation activates the nuclear localization signal of a stress-specific yeast transcription factor. *Embo J* **21**(1-2)**:** 135-144

Page RD (1996) TreeView: an application to display phylogenetic trees on personal computers. *Comput Appl Biosci* **12**(4)**:** 357-358

Shannon P, Markiel A, Ozier O, Baliga NS, Wang JT, Ramage D, Amin N, Schwikowski B, Ideker T (2003) Cytoscape: a software environment for integrated models of biomolecular interaction networks. *Genome Res* **13**(11)**:** 2498-2504

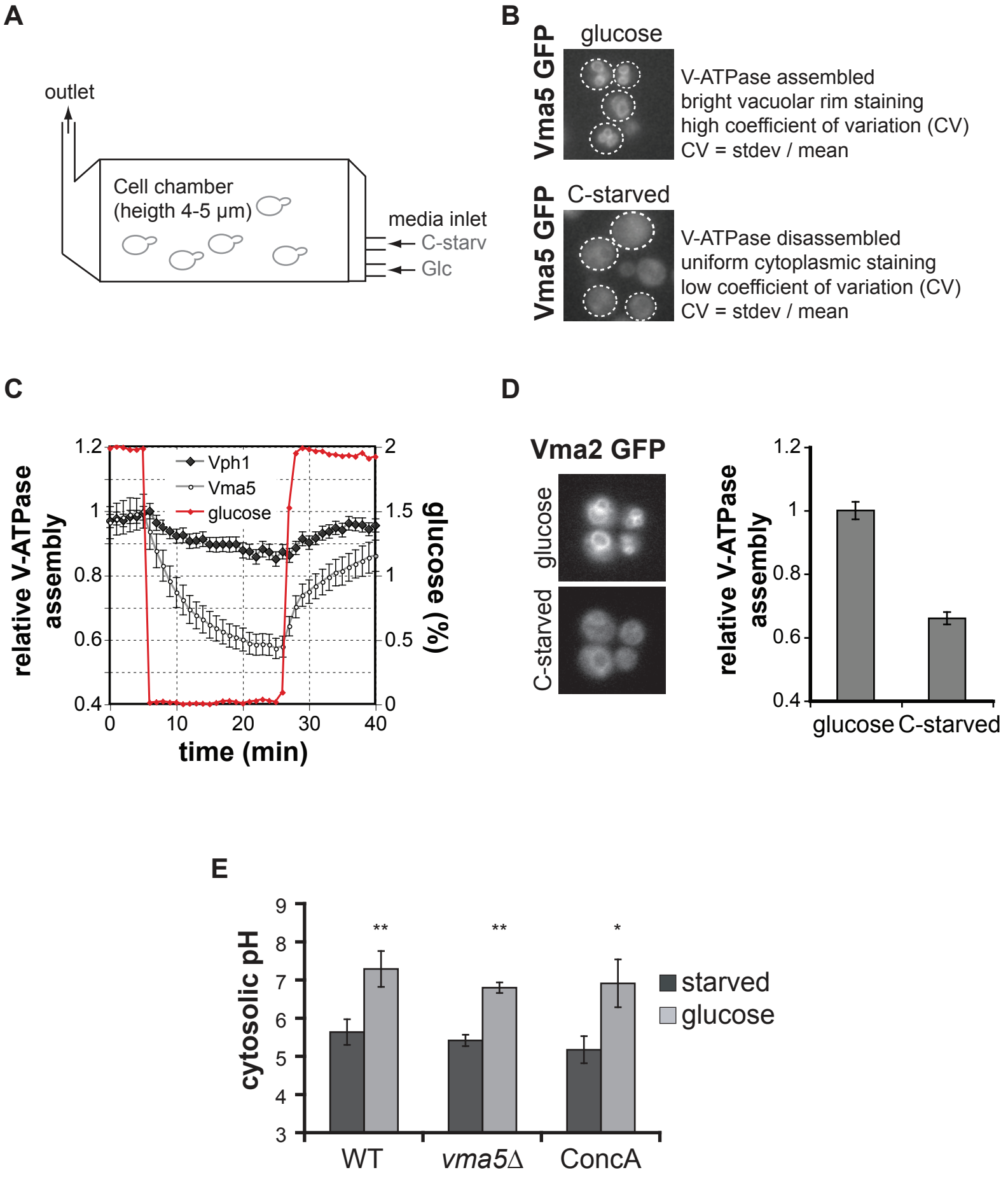

Dechant et al. Figure S1

A

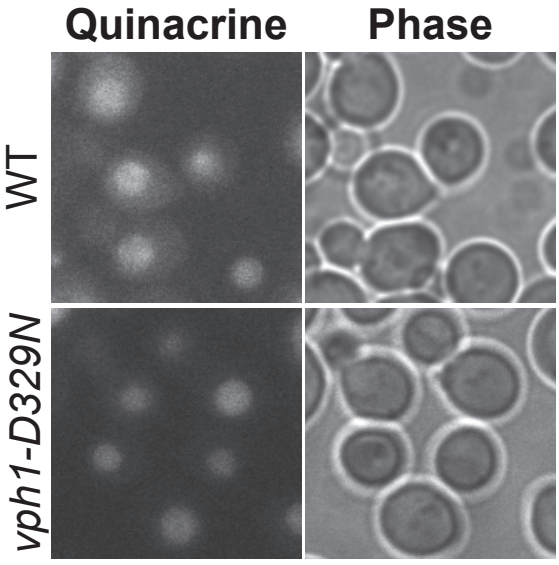

B

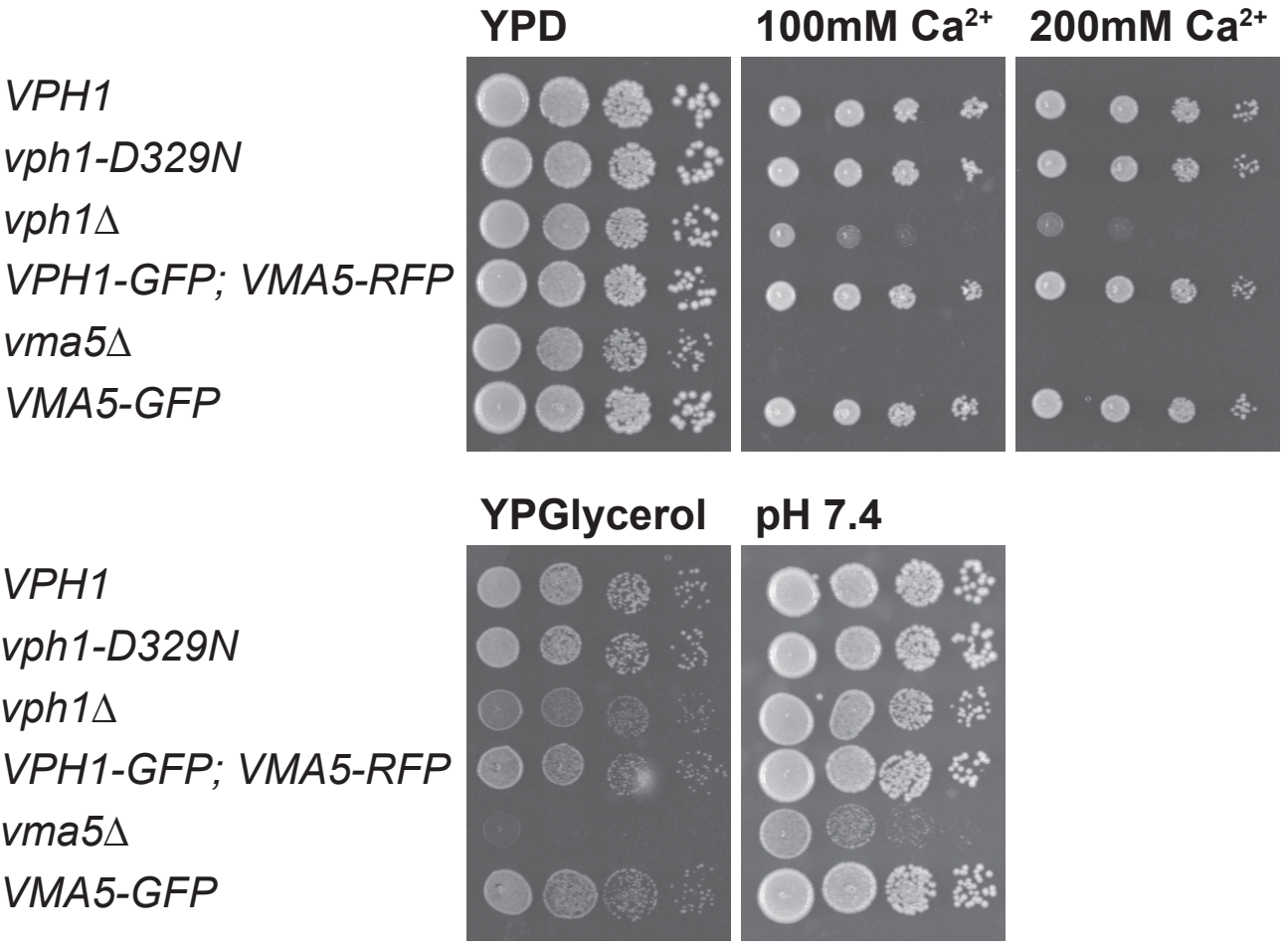

Dechant et al. Figure S2

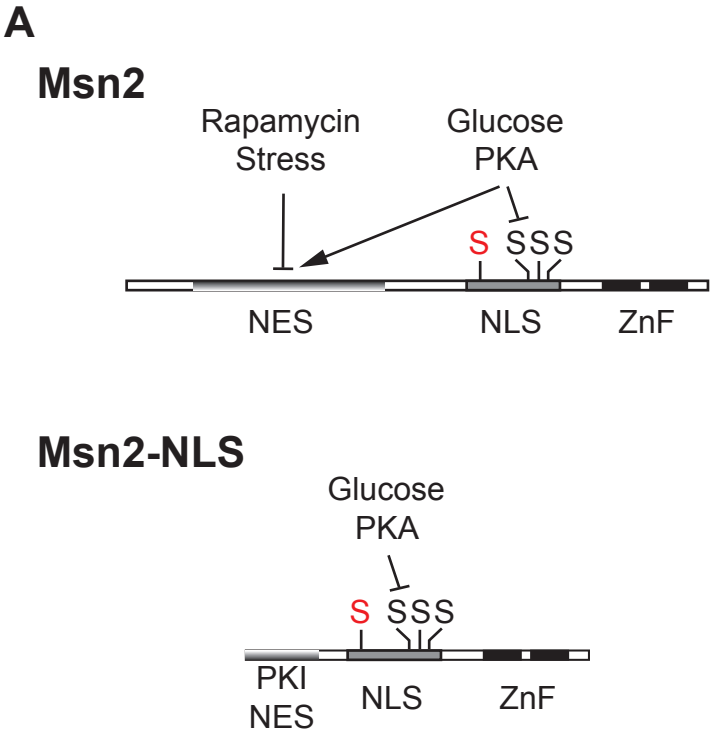

Dechant et al. Figure S3

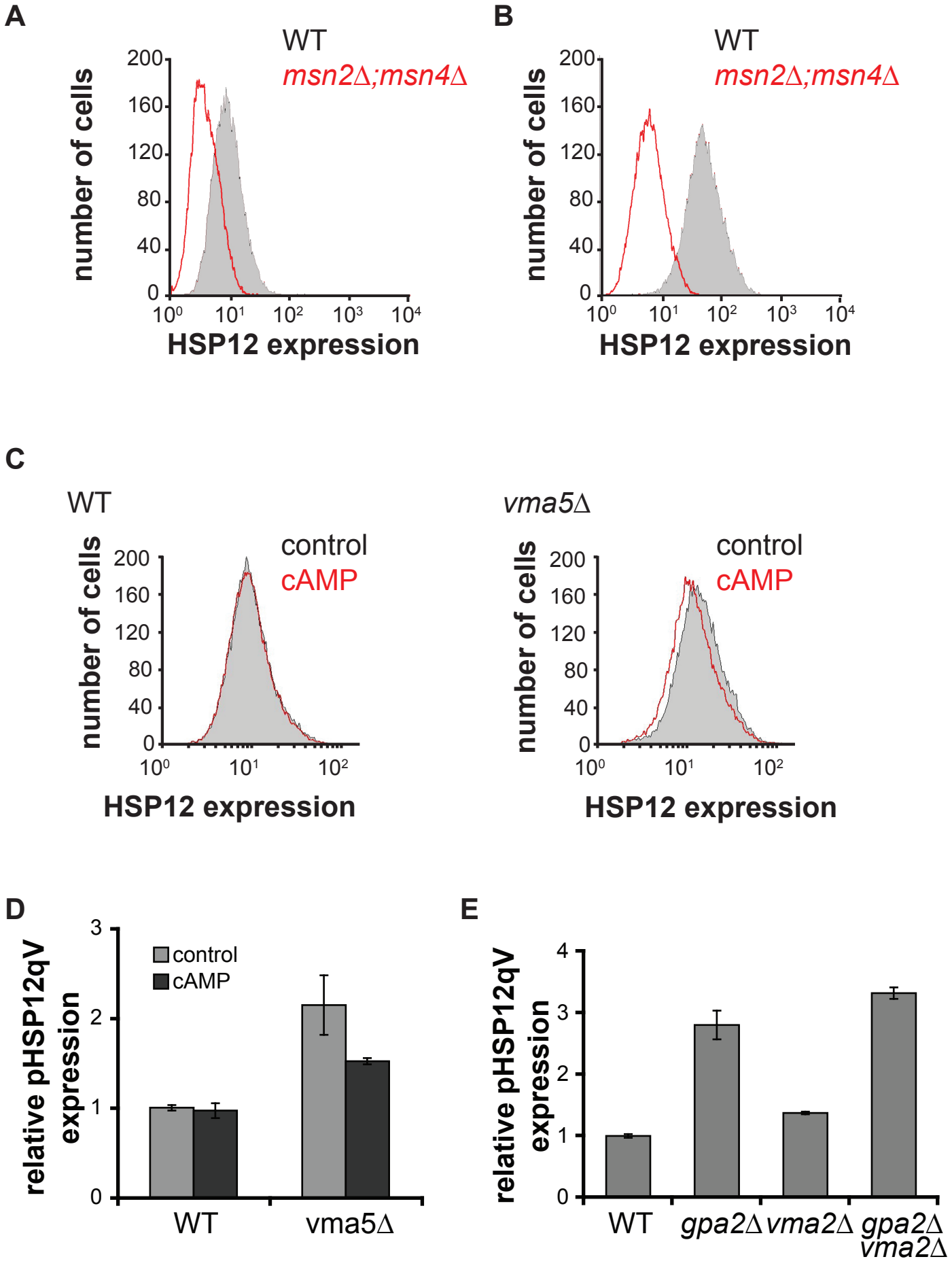

Dechant et al. Figure S4

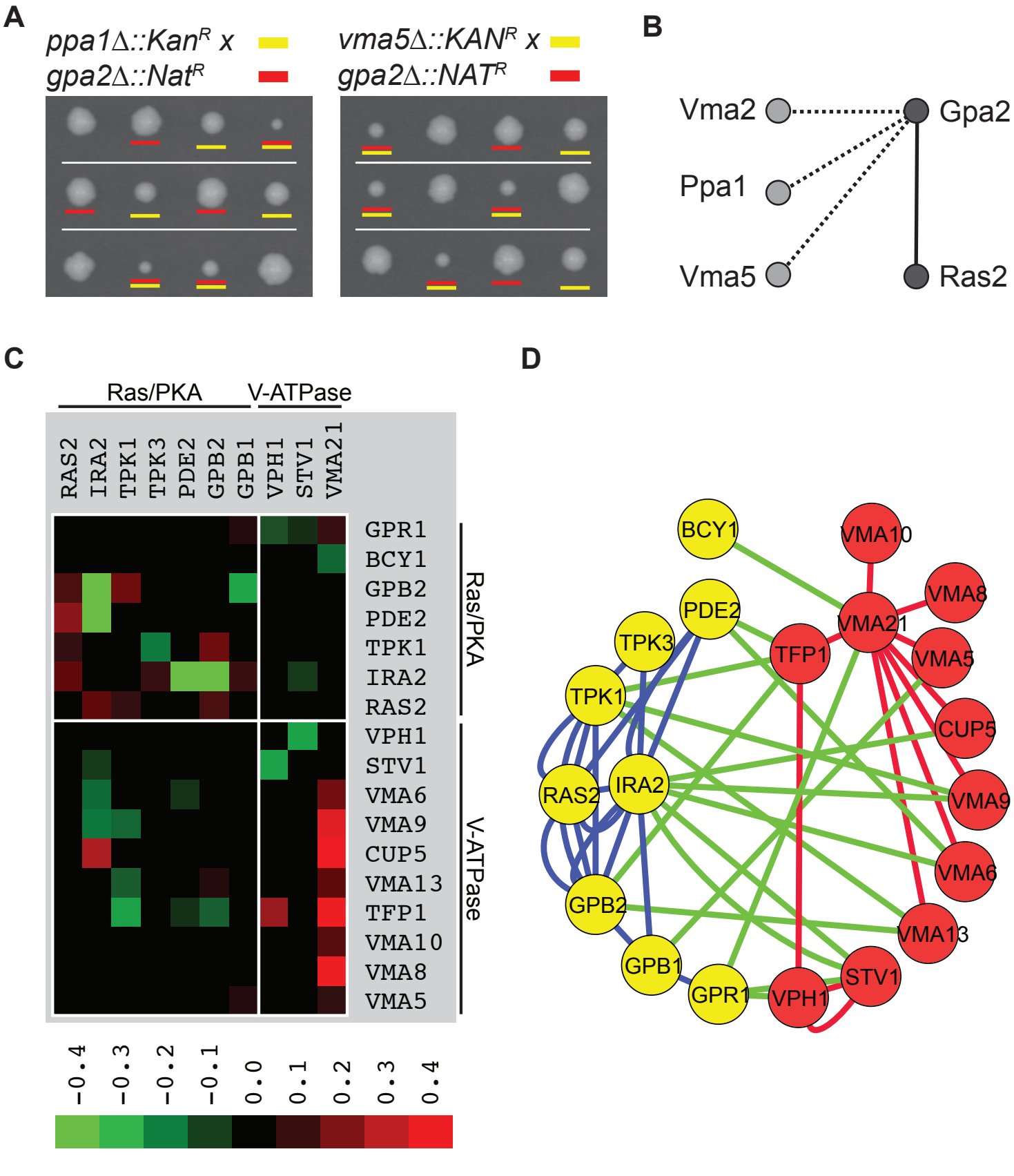

Dechant et al. Figure S5

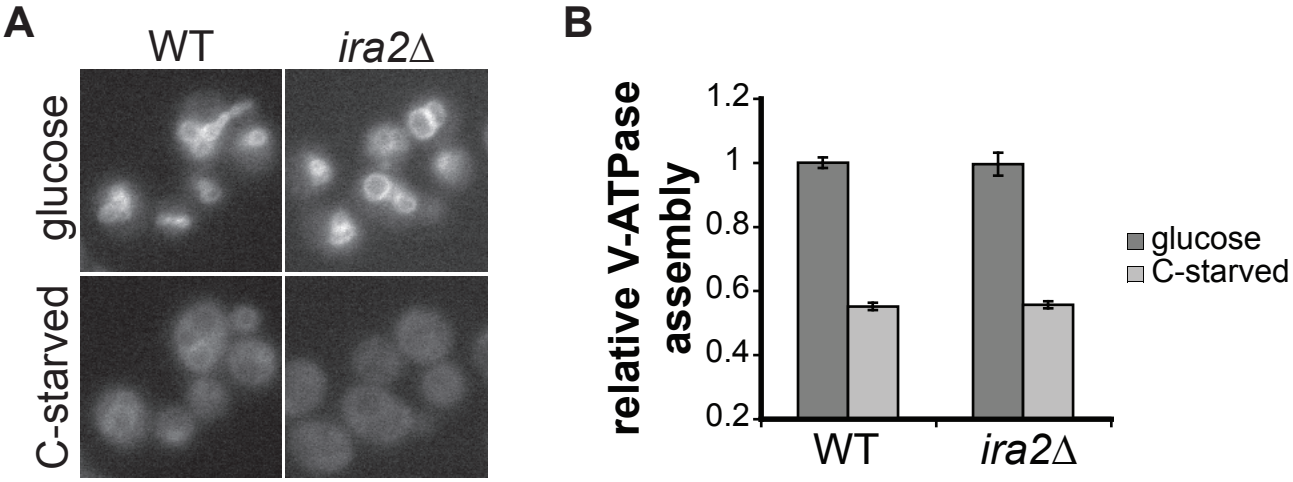

Dechant et al. Figure S6

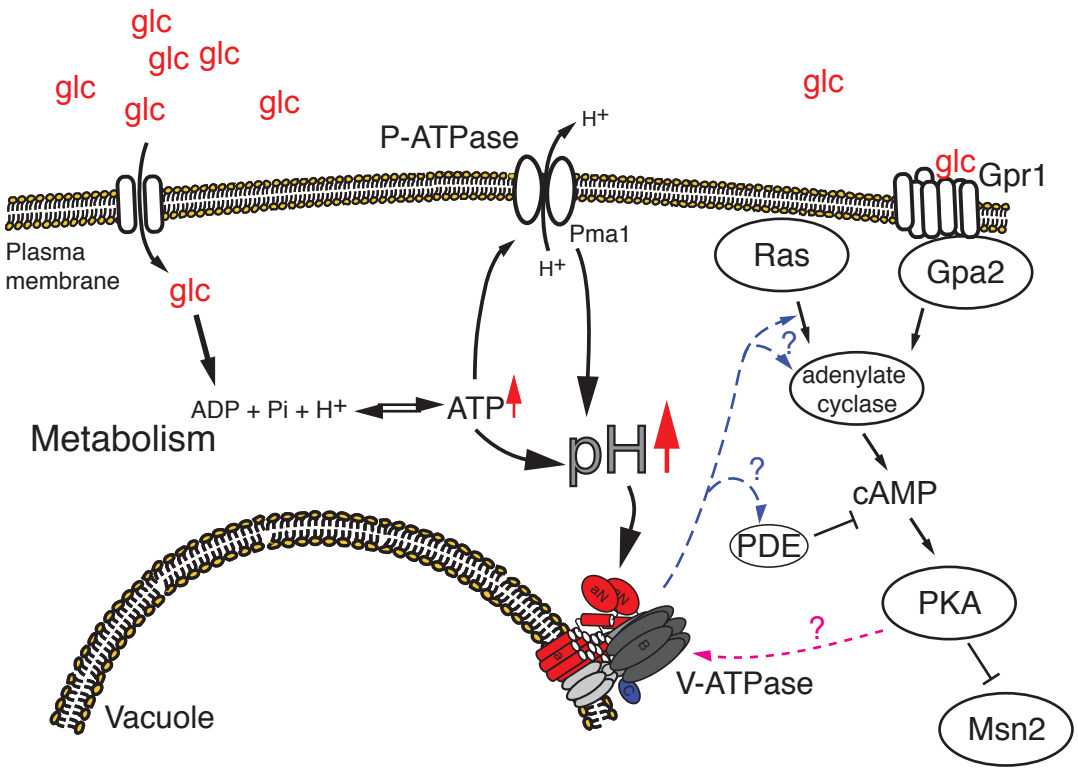

Dechant et al. Figure S7